

AIRBORNE SIMULATION OF LAUNCH VEHICLE DYNAMICS

Christopher J. Miller,^{*} Jeb S. Orr,[†] Curtis E. Hanson,[‡] Eric T. Gilligan[§]

In this paper we present a technique for approximating the short-period dynamics of an exploration-class launch vehicle during flight test with a high-performance surrogate aircraft in relatively benign endoatmospheric flight conditions. The surrogate vehicle relies upon a nonlinear dynamic inversion scheme with proportional-integral feedback to drive a subset of the aircraft states into coincidence with the states of a time-varying reference model that simulates the unstable rigid body dynamics, servodynamics, and parasitic elastic and sloshing dynamics of the launch vehicle. The surrogate aircraft flies a constant pitch rate trajectory to approximate the boost phase gravity turn ascent, and the aircraft's closed-loop bandwidth is sufficient to simulate the launch vehicle's fundamental lateral bending and sloshing modes by exciting the rigid body dynamics of the aircraft. A novel control allocation scheme is employed to utilize the aircraft's relatively fast control effectors in inducing various failure modes for the purposes of evaluating control system performance. Sufficient dynamic similarity is achieved such that the control system under evaluation is configured for the full-scale vehicle with no changes to its parameters, and pilot-control system interaction studies can be performed to characterize the effects of guidance takeover during boost. High-fidelity simulation and flight-test results are presented that demonstrate the efficacy of the design in simulating the Space Launch System (SLS) launch vehicle dynamics using the National Aeronautics and Space Administration (NASA) Armstrong Flight Research Center Fullscale Advanced Systems Testbed (FAST), a modified F/A-18 airplane (McDonnell Douglas, now The Boeing Company, Chicago, Illinois), over a range of scenarios designed to stress the SLS's Adaptive Augmenting Control (AAC) algorithm.

1. INTRODUCTION

Despite well over 50 years of experience in the design, engineering, and operation of launch vehicles, space access remains a high-risk endeavor owing to the extremely high subsystem power densities required to achieve orbital energies. Due to the unique nature of launch vehicle flight mechanics, it is impossible to characterize all subsystem-level interactions present in the actual ascent flight environment prior to the first integrated test of a launch vehicle. In order to mitigate risk to property and the public and to maximize the probability of mission success, some level of subsystem or element testing is mandatory before a space vehicle is committed to fully-integrated flight-testing [1].

The risk of software or algorithm failures is a concern during launch vehicle ascent flight. In particular, the guidance, navigation, and control (GN&C) algorithms can seldom be fully exercised in a relevant flight environment and must be qualified for flight either using incremental unit testing or simulation testing, such as in a hardware-in-the-loop systems integration laboratory [2]. A substantial reduction in risk can be realized by improving the fidelity of the subsystem tests under which the GN&C algorithms are exercised. Such

^{*} Research Engineer, Flight Controls and Dynamics, NASA Armstrong Flight Research Center, Edwards, CA, 93523

[†] Senior Member of the Technical Staff, Dynamics and Control; Draper Laboratory, Huntsville, AL, 35806

[‡] Research Engineer, Flight Controls and Dynamics, NASA Armstrong Flight Research Center, Edwards, CA, 93523

[§] Aerospace Engineer, Control Systems Design and Analysis Branch, NASA Marshall Space Flight Center, AL, 35812

testing, ideally, should stress the avionics hardware and software using environments that are both non-deterministic and indistinguishable from the actual flight environment.

Especially in the case of large space launch boosters, incremental flight-testing is no longer a credible approach to risk reduction during development. Extensive simulation testing, including Monte Carlo analysis, increases confidence in the design but is limited by the so-called epistemic input uncertainties. Anomalies and behaviors caused by “unknown unknowns” are almost always uncovered and characterized during the initial flight-testing of launch vehicles, and the design margins and redundancy typical of human-rated space systems have frequently prevented such anomalies from compromising mission success or crew safety.

The Space Launch System (SLS) (Figure 1) is a human-rated exploration-class launch vehicle currently under development by the National Aeronautics and Space Administration (NASA). The SLS will enable an

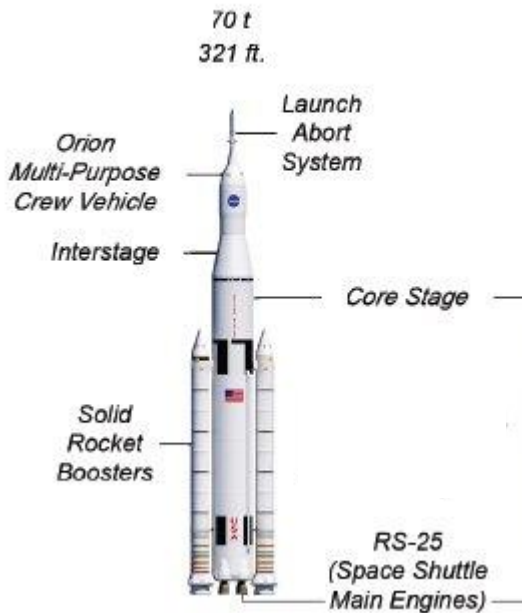


Figure 1. Space Launch System Block I Configuration

unprecedented heavy-lift capability to service payload and mission requirements that cannot be accomplished by current or planned commercial launch vehicles or evolved expendable launch vehicles (EELVs). While the SLS vehicle hardware subsystems, e.g., propulsion, extensively leverage heritage components such as the Aerojet Rocketdyne RS-25E Space Shuttle Main Engine, the massive scale and performance optimization of the integrated vehicle tend to yield formidable challenges for designers of algorithms and flight software. In particular, the flight control system design is challenged by vehicle flexibility and propellant sloshing phenomena and must accommodate a variety of potential subsystem anomalies, such as loss of engine thrust or actuator failures. In order to meet these requirements and increase robustness of the GN&C subsystem, the SLS flight control algorithms contain a novel adaptive control element, Adaptive Augmenting Control (AAC) that had not previously been demonstrated on an operational launch vehicle [3]. The AAC algorithm is the system under test for this experiment. The details of AAC are not presented in this paper. The primary focus of this paper is the construction of a relevant test scenario for AAC and implementation on an aircraft.

In order to reduce risk associated with the SLS flight control algorithms, NASA investigated methods to evaluate AAC in a relevant flight environment. One approach that was explored was the novel concept of simulating the launch vehicle flight environment on a manned aircraft. While there exist diverse capabilities in industry for the use of surrogate aircraft in the simulation of other aircraft, this concept had not previously been demonstrated for a launch vehicle. NASA’s Armstrong Research Center (AFRC)’s workhorse Full Scale Advanced Systems Testbed (FAST), F/A-18 airplane (McDonnell Douglas, now The Boeing Company, Chicago, Illinois), tail number 853, was selected for this effort because it possessed both high performance capability (owing to its military heritage), a modular and extensible avionics platform, and a flight certification and operations paradigm that could support the effort with minimal cost and complexity.

The use of FAST as a surrogate platform for launch vehicle flight control algorithm evaluation required development of a method to simulate launch vehicle dynamics in flight with fidelity and accuracy for evaluating launch vehicle flight software. This effort included simulation of the key drivers for launch vehicle flight control design, including static aerodynamic instability, non-minimum phase bending dynamics, propellant sloshing phenomena, and a zero-lift trajectory. A novel reference model concept and control allocation scheme was integrated with FAST’s proven nonlinear dynamic inversion (NDI) architecture in order to meet these requirements.

The results of these efforts supported the comprehensive Launch Vehicle Adaptive Control (LVAC) flight test campaign to evaluate the SLS AAC algorithm. During these experiments, the SLS flight software was

deployed on the FAST platform and used to control the aircraft in a simulated launch vehicle ascent mode for portions of the SLS ascent trajectory. While the details of the AAC testing and evaluation are outside the scope of this paper, extensive details on this experiment have recently been published [4-6].

The purpose of this paper is to explain the software implementation and the experimental setup for the evaluation of AAC on the FAST vehicle. The structure of the paper is as follows. In Section 2, the architecture, capabilities, and operational approach of the FAST platform are detailed. In Section 3, the choice of the launch vehicle dynamics model and a method of incorporating that model into an airborne research platform are discussed. Simulation and flight-test results from the LVAC campaign are presented in Section 4. Finally, in Section 5, some concluding remarks are provided.

2. FULL-SCALE ADVANCED SYSTEMS TESTBED PLATFORM

An early flight-test evaluation for a technology at a low maturity level can be used to steer and focus the exploration and fuel rapid advances based on real-world lessons learned. One approach for evaluation of new technologies is to exercise the technology in an environment in which increased risk is accepted; that is, where occasional failure is an expected outcome and where failure would not result in loss of life or assets. The FAST platform was designed to facilitate this type of testing for control system technologies, specifically novel algorithms and sensors. Its architecture supports rapid prototyping with quick turnaround in a fly-fix-fly paradigm. The purpose of the testbed is test control technologies that would benefit from flight, obtain data in a relevant environment, and find solutions to the real barriers to innovation at minimal cost with short development and test schedules.

Brief History of Flight Controls Research using F/A-18 Testbeds at Armstrong Flight Research Center

The FAST platform builds on an architecture originally developed for the High-Alpha Research Vehicle (HARV) in the 1980s. The Systems Research Aircraft (SRA) and the Active Aeroelastic Wing (AAW) program later utilized this same architecture, enabling research into variable inceptors, aircraft cooperation, and wing warping for control. The timeline for these research platforms is shown in Figure 2.

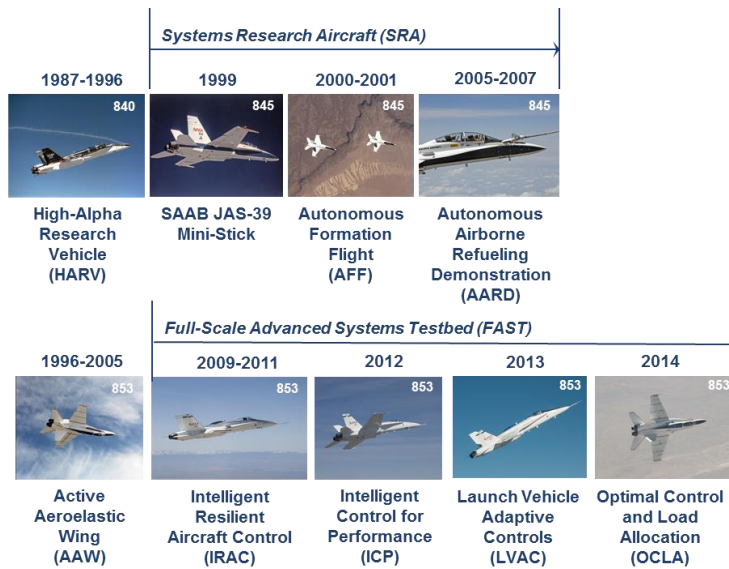


Figure 2. F/A-18 Controls Testbed Timeline

highly adaptive architectures. The LVAC experiment fits well within the original mission for this aircraft. In addition to adaptive controls, research into control technologies that improve aircraft fuel efficiency (Intelligent Control for Performance, or ICP) and technologies that utilize controls to actively prevent structural overload (Optimal Control and Load Allocation, or OCLA) have also been tested on the FAST.

The most current implementation of the architecture is on the FAST vehicle, originally developed to support full-scale piloted testing of adaptive control techniques that hold promise for increased robustness to aircraft failures and environmental uncertainty, but face substantial barriers to their implementation on production vehicles, such as: increased complexity, inadequate verification and validation techniques for adaptive systems, concerns about control-structural interactions, and a lack of understanding about pilot perceptions and interactions with

The most current implementation of the architecture is on the FAST vehicle, originally developed to support full-scale piloted testing of adaptive control techniques that hold promise for increased robustness to aircraft failures and environmental uncertainty, but face substantial barriers to their implementation on production vehicles, such as: increased complexity, inadequate verification and validation techniques for adaptive systems, concerns about control-structural interactions, and a lack of understanding about pilot perceptions and interactions with

Capabilities of the Full-Scale Advanced Systems Testbed

The features of the FAST aircraft facilitate its research mission. High performance research flight control computers have full authority over the vehicle control surfaces and throttle positions. These research systems are linked to the research instrumentation system, enabling novel feedback sensors to be utilized within research control laws. The system can be operated in either quad-redundant or dual-redundant configurations, depending on the computational needs and safety criticality of the experiment. In the dual-redundant configuration, the system is the most flexible, with the ability to host auto-coded Simulink® (The MathWorks, Natick, Massachusetts) and C code. This functionality was key to the success of the LVAC experiment. An additional capability that was added specifically for the LVAC experiment was the ability to provide pilot cueing from the research experiment via the instrument landing system (ILS) needles. This feature enabled the closed-loop testing of the AAC algorithm with the pilot providing the guidance commands. The control surface configuration for the FAST vehicle can be seen in Figure 3.

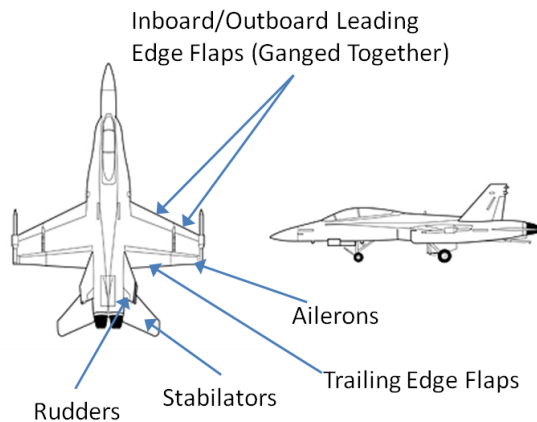


Figure 3. F/A-18 Control Surface Configuration

There are a number of design features that enable rapid prototyping on the FAST. The first is the ability to disengage the research system and safely transition back to the robust production controls. The system automatically monitors aircraft systems and dynamics and automatically reverts to the production control laws in the event of a failure, and the pilot can disengage the experiment at any time and return to a well-known control configuration.

While the full F/A-18 flight envelope is accessible for research, it requires substantial testing and verification for closed-loop control experiments. The protected flight envelope (Figure 4) facilitates rapid prototyping using the FAST. Limiting the allowable airspeed and altitude envelope for research experiments mitigates the risk of overloading the structures of the aircraft. The structural strength of the airframe, the ability to revert to the robust production control laws, and the limited research envelope allow researchers to experiment with advanced techniques without putting the pilot or the aircraft at undue risk, and allow for reduced verification and validation (V&V) testing prior to flight.

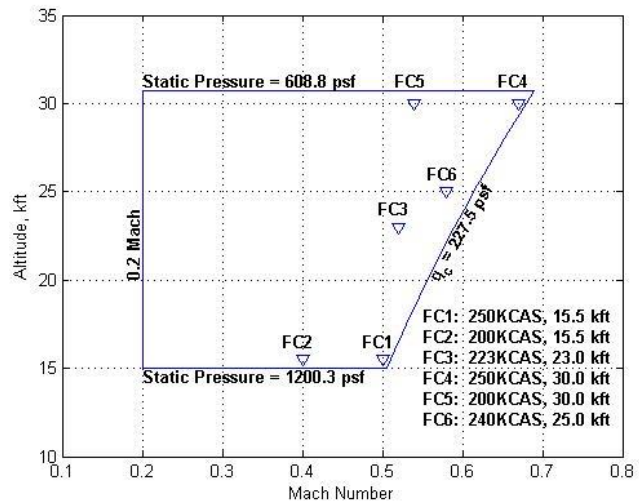


Figure 4. Research Envelope

Flight-testing AAC on an aircraft offered a number of other advantages over other possible platforms. The low cost per flight hour of the F/A-18 airplane as compared to rocket platforms facilitated the gathering of hours of flight data in a wide variety of test conditions. The platform is configurable in-flight between test points using pilot-selectable configuration parameters. This in-flight test flexibility enabled efficient test planning and back-to-back comparisons of algorithm performance for a wide array of test scenarios. The presence of a pilot in the aircraft allowed for evaluation of the interactions between the AAC algorithm and a human pilot [6]. The research flight control computers on the FAST facilitated testing with the actual SLS production flight software prototype. The LVAC experiment exercised the same source code executing on the FAST research computers as is expected to eventually execute on the real SLS hardware. The protected

envelope shown in Figure 4 along with the mature experiment monitoring and disengage functionality designed into the FAST platform facilitated an accelerated flight certification process which enabled the aggressive project schedule. In addition, the existing high-fidelity FAST hardware-in-the-loop simulation (HILS) facility was a crucial element, allowing the team to progress quickly through experiment software verification testing and uncover a number of anomalies in the flight code. Fully integrated with the production mission operations facility via high-speed network and communications interfaces, the HILS facility was also used to practice the LVAC test missions with the control room prior to executing the flights.

Full-scale Advanced Systems Testbed Configuration for the Launch Vehicle Adaptive Control Experiment

It is not immediately obvious that a fighter aircraft can present a relevant test environment for software designed for a rocket. However, the features of the experiment design are able to directly support the maturation of the AAC software for application to the SLS program. For example, the flight trajectory was designed using a zoom climb to 35-deg nose-high pitch attitude followed by pitch-over at a constant pitch rate of 0.75 deg/sec. This trajectory is similar in shape and timing to the SLS gravity turn trajectory prior to booster separation. The aircraft is able to simulate ~75 seconds of the gravity turn surrogate maneuver, which is a substantial percentage of the nominal ~120 seconds from launch to booster separation for SLS. The similar dynamic characteristics of the guidance commands implies that the SLS guidance interface and steering logic can be exercised on the F/A-18 airplane without modification. An example of the test trajectory with a failure scenario is shown in Figure 5.

In addition to the trajectory shape and timing, the pitch axis dynamic response to guidance commands for the F/A-18 airplane is matched to that of the predicted SLS response. This matching is accomplished through the use of the NDI controller designed for use with FAST experiments [7, 8]. The NDI effectively inverts the known bare airframe rigid body dynamics of the F/A-18 airplane and forces the F/A-18 airplane to track the dynamics of an onboard reference model of the SLS. An accurate inversion is possible because the desired dynamics of the SLS (both rigid-body and flexible modes) are within the achievable bandwidth of the F/A-18 airplane, and the NDI algorithm utilizes an extensive flight-correlated database of F/A-18 dynamic response. For the LVAC experiment, the multiple pitch control effectors of the F/A-18 airplane were used to separately generate the rigid body and elastic components of the SLS dynamics, allowing closure of the control loop physically outside the aircraft. Specifically, the flexible modes are generated through the use of symmetrical aileron deflections and the other surfaces are used for the rigid-body dynamics.

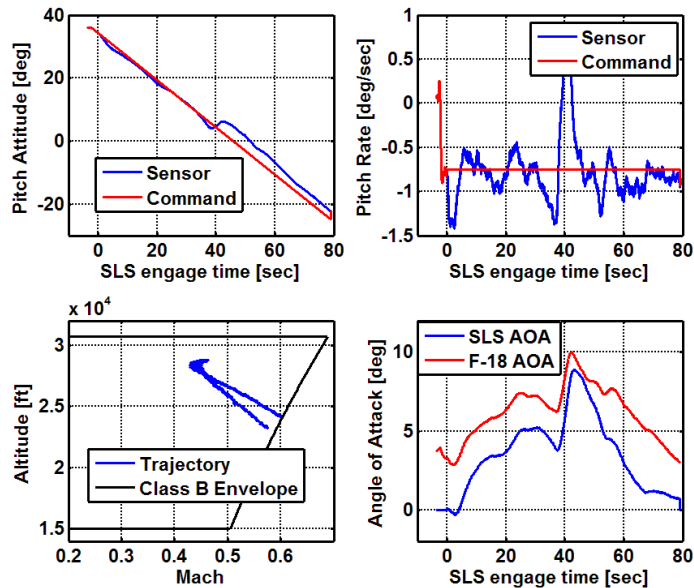


Figure 5. Gravity-Turn Surrogate Trajectory Example

In the development of the experiment, it was taken into account that the F/A-18 airplane is flying a substantially different Mach, altitude, and dynamic pressure profile than those of the SLS. The structure of the reference model is such that the translational state of the aircraft is decoupled from the reference pitch attitude dynamics, implying that matching of the translation state is not achievable primarily due to the lower Earth-relative velocity, which does preclude testing of some components of the SLS autopilot. These components of the software are mature, however, and have heritage from previous flight tests and legacy vehicles and were outside of the scope of the LVAC test.

The lift curve slope of the F/A-18 airplane is substantially different from that of the SLS vehicle, which results in differences in the angle-of-attack profiles. As a result, the actual angle-of-attack measurement from the F/A-18 airplane cannot be used directly within the SLS model for simulation of aerodynamic instability;

rather, an estimate of the angle of attack of the SLS must be generated within the reference model. This quantity, based on the calculated vehicle lateral velocity and the reference pitch attitude error, is used within the reference model of the SLS for computation of the aerodynamic moments. The shape of the F/A-18 angle of attack profile, excluding the trim lift effects, however, matches the desired shape of the SLS reference trajectory very well (Figure 5).

For test point development, the excellent characterization and tight error tracking of the NDI inner loop allowed the FAST aircraft response to be modeled as a linear parameter varying second-order plant with a time delay. While the aircraft response dynamics are primarily a function of dynamic pressure, which continuously varied throughout the LVAC test trajectory, the variation was very repeatable and could therefore be modeled as a function of time. The NDI minimized this variation and simplified the modeling and analysis of the SLS test conditions.

3. LAUNCH VEHICLE MODEL IMPLEMENTATION FOR LAUNCH VEHICLE ADAPTIVE CONTROL

Space Launch System Reference Model Dynamics

For flight control analysis, the dynamics of an ascending launch vehicle are typically modeled by time-varying linear models with nonlinear subsystem models such as actuators. For final verification of the design, the vehicle ascent is simulated using a high-fidelity dynamics code that includes all relevant nonlinear effects. Constructing a linear representation of a launch vehicle, however, is a formidable modeling task. Capturing the mutual coupling of the rigid body, engines, sloshing propellant, and elastic dynamics requires the solution of an implicit set of coupled linear ordinary differential equations in a descriptor form [9]. The underlying dynamic models can include from a few dozen to several hundred degrees of freedom.

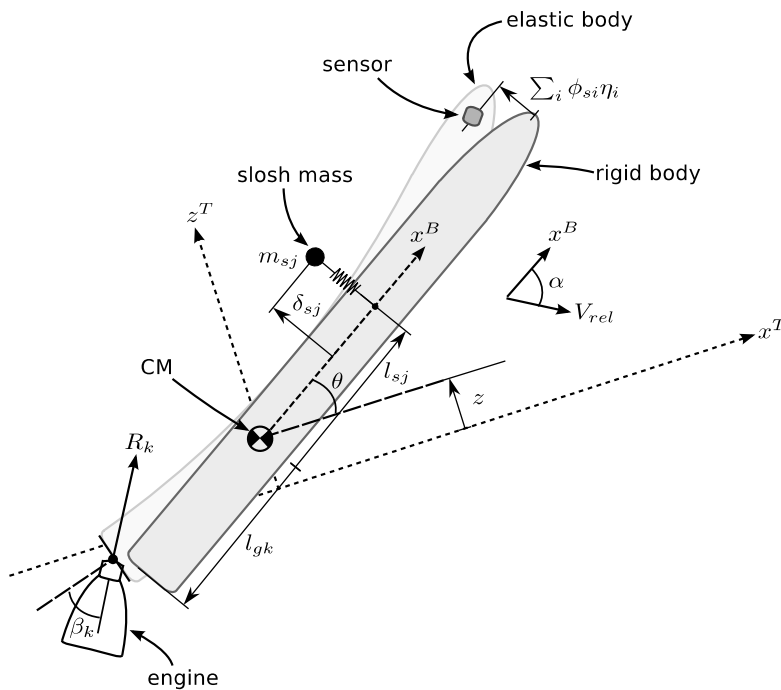


Figure 6. Launch Vehicle Trajectory Frame

The in-flight dynamic reference model for the LVAC experiment was based upon a quasi-linear perturbation flight mechanics formulation derived from a simplified, time-varying version of the Frequency Response Analysis and Comparison Tool Assuming Linearity (FRACTAL) model [9, 10]. The FRACTAL is the primary design and assessment tool for SLS ascent flight control [3], and its rigorous verification history allowed incorporation of the relevant dynamic models into the LVAC flight software without requiring extensive simulation development or supplemental verification activities. The LVAC implementation of FRACTAL was truncated to the vehicle pitch plane, since the test objectives could be achieved by simulating only the longitudinal axis. Certain effects modeled in FRACTAL but not relevant to the control system evaluation, such as aeroelasticity, were omitted from the LVAC

implementation.

In the FRACTAL model, the vehicle is linearized with respect to an accelerating trajectory centered at the vehicle nominal center of mass location (Figure 6). Since the reference trajectory is considered to be a gravity turn (zero-lift) trajectory, the attitude deviation θ and the velocity normal to the trajectory \dot{z} can be used to construct the angle of attack.

The launch vehicle degrees of freedom simulated on board the aircraft include rigid-body rotation and translation, 6 to 10 bending generalized coordinates, two sloshing propellant degrees of freedom corresponding to the fundamental lateral oxidizer and fuel modes, and the nonlinear dynamics of all six vectored engines. The scalar motion equations for bending, rotation, translation, slosh, and engines are given by Equations (1) through (5), respectively:

$$\ddot{\eta}_i + 2\zeta_{bi}\dot{\eta}_i + \omega_{bi}^2\eta_i = \sum_k \left((S_{nk}\phi_{gki} - J_{nk}\psi_{gki})\ddot{\beta}_k + R_k\phi_{gki}\beta_k \right) - \sum_j m_{sj}\phi_{sij}\ddot{\delta}_{sj} \quad (1)$$

$$J_{yy}\ddot{\theta} = - \sum_j m_{sj}l_{sj}\ddot{\delta}_{sj} - \sum_k \left((l_{gk}S_{nk} + J_{nk})\ddot{\beta}_k + l_{gk}R_k\beta_k \right) - \sum_i \sum_k R_k\phi_{gki}\eta_i + \bar{q}Sl_a C_{N\alpha}\alpha \quad (2)$$

$$m_T\ddot{z} = - \sum_j m_{sj}\ddot{\delta}_{sj} + \sum_k \left(S_{nk}\ddot{\beta}_k + R_k\beta_k \right) + m_T\bar{g}\theta + \bar{q}SC_{N\alpha}\alpha \quad (3)$$

$$\ddot{\delta}_{sj} + 2\zeta_{sj}\omega_{sj}\dot{\delta}_{sj} + \omega_{sj}^2\delta_{sj} = -\ddot{z} - l_{sj}\ddot{\theta} + \bar{g}\theta - \sum_i \phi_{sij}\ddot{\eta}_i \quad (4)$$

$$J_{nk}\ddot{\beta}_k + C_{nk}\dot{\beta}_k + K_{nk}\beta_k = S_{nk}(\ddot{z} - \bar{g}\theta) - (l_{gk}S_{nk} + J_{nk})\ddot{\theta} + \sum_i (S_{nk}\phi_{gki} - J_{nk}\psi_{gki})\ddot{\eta}_i + g_k \quad (5)$$

The rigid-body parameters are the vehicle total mass and pitch axis inertia m_T and J_{yy} , as well as the trajectory acceleration \bar{g} . The sloshing modes are described by their mechanical equivalent sloshing mass, mass location, frequency, and damping m_{sj} , l_{sj} , ω_{sj} , ζ_{sj} . Likewise, the bending dynamics are described by finite element model modes with frequency and damping ω_{bi} , ζ_{bi} and mode shape and slope eigenvectors ϕ_{gki} , ψ_{gki} at the k^{th} engine gimbal. Each engine is described by its location l_{gk} and its first and second moments of inertia about the gimbal point S_{nk} , J_{nk} . Each engine has a thrust R_k and an angle β_k with respect to null. Finally, the vehicle aerodynamics are modeled using a normal force coefficient $C_{N\alpha}$ and a center-of-pressure location l_a .

Recognizing that the reference trajectory $\theta = z = 0$ is a zero-lift trajectory (where $\alpha = 0$), these motion equations can be coupled to the actual rigid-body airframe by assuming that the actual (sensed) trajectory error $\hat{\theta}$ is also with respect to a zero-lift trajectory. In this mechanization, Equation (2) is solved to yield the desired rigid-body pitch angular acceleration. The desired acceleration is used to command the aircraft dynamic inversion scheme in real time, while the actual aircraft pitch attitude state $\hat{\theta}$ is used in equations (3) through (6) to propagate the equations of motion. Due to limitations in the performance and subsystems of the F/A-18 airplane (particularly fuel sump pickup and turbine lubrication requirements), it is generally not possible to fly a zero-lift trajectory for an extended period of time. As mentioned previously, however, the F/A-18 airplane is capable of maintaining a trajectory having a constant pitch rate nearly the same as that used for the operational launch vehicle boost profile. In addition, the total aircraft air-relative velocity and the accumulated aircraft normal velocity will differ substantially from the actual launch vehicle values, since the aircraft thrust-to-weight ratio is less than unity. In order to maintain dynamic similarity in the face of these constraints and still simulate an unstable short-period longitudinal mode, an internal estimate of angle of attack is formed using the method shown in Equation (6):

$$\alpha = \hat{\theta} - \frac{\dot{z} + v_w}{V} \quad (6)$$

where \dot{z} and v_w are derived internally through integration of Equation (3) and an internal winds model, respectively. In this manner, the value of angle of attack used to propagate the dynamics is based upon both the actual sensed vehicle attitude (matched well by the F/A-18 airplane) and an internal model of the translational dynamics (not matched well by the F/A-18 airplane). The use of both an internal and external state to compute the angle of attack implies that the control system performance can be evaluated using both severe simulated wind loading (via v_w) and actual flight day environments, such as turbulence.

Finally, the parasitic effects of bending on a launch vehicle flight control system are of primary importance. The sensed rate is derived from the generalized velocity in Equation (1) as shown in Equation (7):

$$\dot{\theta}_s = \dot{\theta} + \sum_m \sum_i \psi_{smi} \dot{\eta}_i \quad (7)$$

where ψ_{smi} is the mode slope eigenvector component of the i^{th} mode at the m^{th} sensor. On many large launch vehicles, including SLS, these multiple rate gyros are optimally blended to reduce the effects of bending. The F/A-18 airplane, however, senses rate at a single location and the airframe bending modes are separated from the frequencies of interest to SLS. A scheme was devised wherein the total commanded acceleration could be partitioned into its rigid-body and elastic components. These two components were used to command a set of control surfaces separate from those used for rigid-body feedback control, thereby allowing the experiment to demonstrate bending stabilization using a physical mechanism (outside the aircraft) rather than within the software.

The reference dynamics [Equations (1) through (7)] are integrated using a fourth order Runge-Kutta algorithm and parameters indexed with respect to simulated trajectory time. The linear portion of the actuator dynamics are also run in discrete time along with a detailed failure model that includes the ability to inject, for example, hard-over and fail-in-place faults in the thrust vector control (TVC) system.

Since the bending dynamic response varies in time as mass is consumed, multiple sets of finite element modes are propagated and modal transitions are accomplished using quadratic inequality constrained least-squares (LSQI) initialization, which determines the generalized coordinates such that physical displacement, velocity, strain, and kinetic energy are continuous across each transition [9]. Various disturbance simulation capabilities are also implemented, including a parametric wind shear and bias angular acceleration models.

Software Implementation on the Full-scale Advanced Systems Testbed

The LVAC experiment was hosted on the FAST vehicle within the Airborne Research Test System (ARTS), which are dual-redundant systems with three single-board computers (SBCs) in each system. The experiment input/output, error checking, and signal voting are all handled in the first SBC while up to four experiments can be hosted in each of the other two SBCs. The base computation rate for the FAST research computers is 160Hz, to enable tight coupling to the production F/A-18 flight control computers, which execute at that rate. The LVAC experiment placed a significant computational burden on the 900-MHz PowerPC, thus it was hosted as the only experiment in single-board computer number two. In addition to making LVAC the sole experiment, other design features were required to allow sufficient computational margin so as to complete all necessary control law functions without overrunning the 3.25 milliseconds of allotted computational time for ARTS experiments. The first was to stagger the SLS Flight Control System updates and the aerodynamic table lookups in the NDI. The SLS FCS was executed on even 80-Hz frames while the table lookups for computing surface effectiveness were executed on odd 80-Hz frames. The ARTS software was also modified to allow the research experiment execution to start earlier than previous experiments and the available stack memory allotment was increased for LVAC. The initialization function for SLS FCS and the actual FCS needed to be staggered as well at the start of the experiment to allow it to complete execution in the allotted time.

Figure 7 depicts the top-level layout for the LVAC experiment. The approximate gravity turn pitch rate maneuver provides the guidance commands to the SLS FCS. The tracking errors for these commands are computed from the production F/A-18 airplane sensed rates and attitudes and are used by both the FCS and the reference modes. The SLS FCS block contains the prototype SLS flight software implemented in the Simulink® via the use of an *S-Function* wrapper, which enabled the interfaces with the existing NDI

Simulink® experiment and the auto-coding for the ARTS VxWorks operating system. The outputs from the SLS FCS are used within the SLS reference dynamics which are run at the full 160-Hz rate of the ARTS.

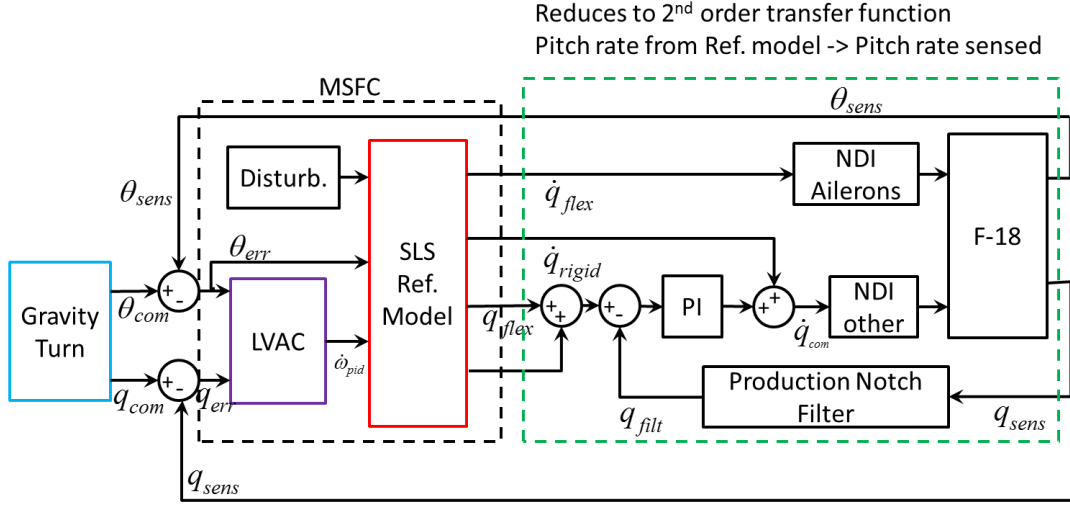


Figure 7. Full-scale Advanced Systems Testbed Experiment Software Architecture

Pitch angular rate and acceleration from the SLS reference model are used as inputs to the NDI controller as the desired F/A-18 dynamics. The rigid-body dynamics of the airframe with estimated aircraft inertia \mathbf{J}_a are approximated as shown in Equation (8):

$$\mathbf{J}_a \dot{\omega}_c + \omega^\times \mathbf{J}_a \omega = q_i S \mathbf{A} \mathbf{x} + q_i S \mathbf{B} \mathbf{u} \quad (8)$$

where the angular acceleration has been replaced by the commanded angular acceleration. The quantities q_i and S are the dynamic pressure and reference area scaling factors, respectively.

The commanded angular acceleration can be separated into the flexible- and the rigid-body contributions, and the matrix \mathbf{B} and the input \mathbf{u} can be partitioned into two sets of surfaces used for generation of the rigid- and flexible-mode contributions as shown in Equation (9).

$$\mathbf{J}_a \left(\begin{bmatrix} \dot{p}_c \\ \dot{q}_{cr} \\ \dot{r}_c \end{bmatrix} + \begin{bmatrix} 0 \\ \dot{q}_{cf} \\ 0 \end{bmatrix} \right) + \omega^\times \mathbf{J}_a \omega = q_i S \mathbf{A} \mathbf{x} + q_i S \mathbf{B}_r \mathbf{u}_r + q_i S \mathbf{B}_f \mathbf{u}_f \quad (9)$$

Equation (9) is then solved for each of the necessary surface commands using the sensed angular rate $\hat{\omega}$ and state estimate $\hat{\mathbf{x}}$, as shown in Equations (10 and (11).

$$\mathbf{u}_r = \mathbf{B}_r^\dagger \left\{ \frac{1}{q_i S} \left(\mathbf{J}_a \begin{bmatrix} \dot{p}_c \\ \dot{q}_{cr} \\ \dot{r}_c \end{bmatrix} + \hat{\omega}^\times \mathbf{J}_a \hat{\omega} \right) - \mathbf{A} \hat{\mathbf{x}} \right\} \quad (10)$$

$$\mathbf{u}_f = \frac{1}{q_i S} \mathbf{B}_f^\dagger \mathbf{J}_a \begin{bmatrix} 0 \\ \dot{q}_{cf} \\ 0 \end{bmatrix} \quad (11)$$

The inversion of the control coefficient matrices is accomplished using the standard Moore-Penrose inverse; the commanded pitch angular acceleration is derived via solution of Equation 2 and the elastic angular acceleration is derived from Equation (7).

At experiment engagement, the NDI is in full control of the aircraft. A supplemental autopilot sequencer levels the wings and initiates the pitch-over maneuver. After approximately 3 seconds, and exactly one 160-hz frame before control is transitioned to the SLS control laws, the integrators and filters are initialized

and begin updating their states. The inputs to the SLS control laws are faded from a zero error state to the actual error state over a 0.5-second time frame. This transient free switch eliminates any rapidly varying inputs and prevents the AAC algorithm from being adversely affected by any residual error in the trajectory setup from the 3 seconds that the NDI was in full control. The timing and execution of this handoff from the F/A-18 production control laws, to NDI, was crucial in ensuring the validity of the F/A-18 flight-test results and their applicability to the production vehicle. Different portions of the boost trajectory were simulated with different failure and test scenarios, depending on the critical phase of the launch. Depending on the test scenario, a different start time for the boost trajectory was used for performing the gain scheduling and reference model table lookups.

4. FLIGHT-TEST RESULTS

The differences between the preflight predictions and flight-test results were surprisingly small. The nominal test cases and then ones with anomalies at low frequencies were almost identical in-flight to the simulation predictions

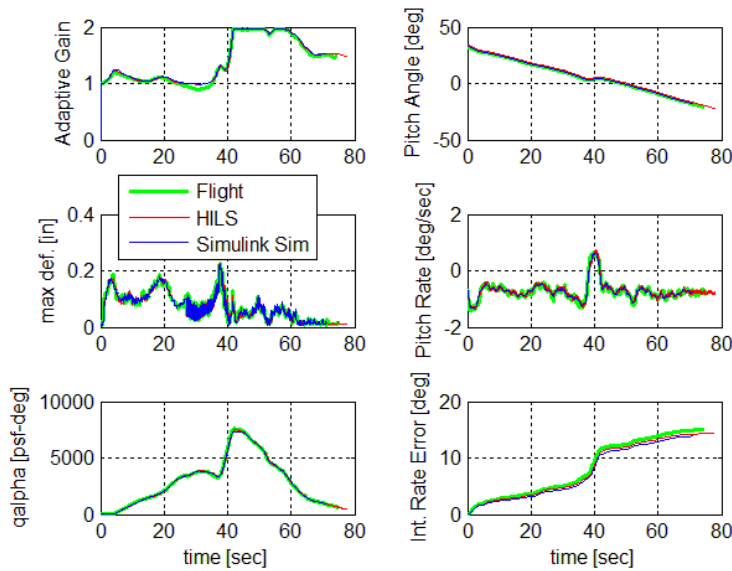


Figure 8. Simulation-to-Flight Comparison with an Actuator Hardover

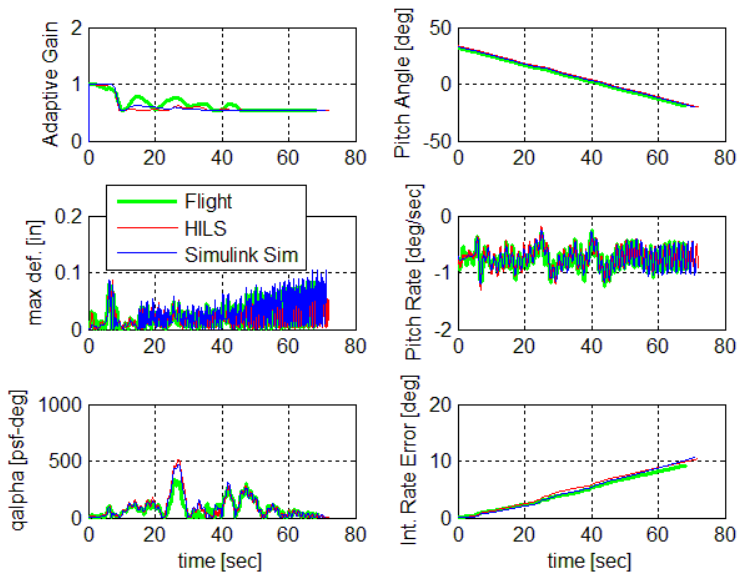


Figure 9. Comparison with a Simulated Slosh Instability

simulation predictions (Figure 8). It can be seen that the behavior of the adaptive controller is very similar in all three environments (desktop simulation, hardware-in-the-loop simulation, and flight data). The performance of the NDI forces the aircraft to track pitch attitude and rate of the reference model very well, and even the integrated error over the entire trajectory is well predicted by the simulations. This case is a representative example of the kind of agreement seen for all of the low-frequency failure scenarios and nominal test cases.

However, not all of the flight results exactly matched the preflight simulations. The most difficult test cases from an NDI tracking perspective were the higher frequency test cases involving simulated SLS slosh and structural modes. The structural modal responses were simulated on the F/A-18 airplane through the use of symmetrically deflected ailerons. This control configuration is not used by the production aircraft and is therefore not well characterized in the simulation. It is not surprising, then, that there were errors in the

simulation predictions for those test cases; much larger pitch rates were generated in flight than were predicted by simulation. This behavior is a result of the ailerons having more effective pitch moment than originally predicted, yielding, in one case, a more unstable simulated structural mode. The adaptive control behavior was the same, however; as such, the test case met the intent of the flight objective, which was to validate the adaptive controller in the presence of unstable bending dynamics.

A more interesting difference between simulated and flight behavior did not immediately yield an obvious explanation. The test cases with simulated SLS slosh instabilities (Figure 9) exhibited a slow oscillation, or limit cycling, of the adaptive gain. While this limit cycle behavior had been predicted prior to flight, it occurred at a much lower frequency and did not readily appear in either simulation. The underlying dynamics in all three cases are very similar; however, upon close inspection, it was found that a small amount of additional phase delay was apparent in the flight data. While not a significant contributor to the overall dynamics, this delay was found to have exerted a significant effect on the adaptive controller response. Upon further examination, these results motivated a small design modification for the final SLS implementation.

5. SUMMARY

The idea that an aircraft can represent a valid and cost-effective test platform for space and launch technologies opens the door to testing opportunities that would otherwise be infeasible due to cost and schedule constraints. This experiment is a first step and shows the utility of such an approach. All technology development programs are alike in that cost-effective test environments that facilitate technology maturation are invaluable. Platforms such as the Full-scale Advanced Systems Testbed are a resource that can be leveraged by a wide array of development activities, even ones that, at first, seem to have very different applications. New ways of thinking and consideration of “outside of the box” ideas and techniques is essential to aggressive pursuit of ever more complex and capable technologies while minimizing cost. A coordinated investment in these test environments is necessary to accomplish the bold and inspiring goals of NASA’s Agency-level mission.

The Launch Vehicle Adaptive Control (LVAC) flight experiment has shown that a high performance fighter aircraft on an aggressive trajectory can simulate a dynamic environment similar to that of a launch vehicle during a boost trajectory. A successful flight-test campaign demonstrated, for the first time, the use of a surrogate aircraft to simulate the dynamics of an orbital launch vehicle for the purposes of flight software and algorithm characterization, evaluation, and test. The resultant test data continue to be used extensively by the Space Launch System flight control design team to tune algorithm parameters and enhance the robustness of the design.

The LVAC experiment has illustrated that with careful evaluation of the goals and objectives of a test and evaluation effort, an aircraft can represent a low-cost option for the maturation of software ultimately designed for a launch vehicle. By pairing mature test assets with innovative technologies, valuable insight and experience can be gained about the technology under test with minimum risk, even in the face of an aggressive schedule.

6. ACKNOWLEDGMENTS

The authors extend their appreciation to those who have supported the initial and will support the continued development of the Adaptive Augmenting Control (AAC) algorithm. We include Mark Whorton for casting the vision and guiding the initial research toward the development of adaptive control for launch vehicles. Also Charlie Hall, Space Launch System (SLS) Guidance, Navigation, and Control (GN&C) Lead, whose efforts were critical in advocating for the maturation of this technology and for its inclusion, when appropriate, as part of the SLS baseline autopilot design. Several other members of the NASA community also served key roles in being able to allocate time during the algorithm’s initial development phase, providing expert review, gaining support within the NASA community, and obtaining resources toward the flight characterization experiment: including John Hanson, Don Krupp, Mark Jackson, Steve Ryan, Dave Edwards, Jimmy Compton, Jimmy Jang, Mark West and Garry Lyles. In addition, the authors thank our partners Neil Dennehy, Ken Lebsock, Vicki Regenie, Jim Stewart, Steven Gentz, Patricia Pahlavani, and Pam Sparks of the NASA Engineering and Safety Center (NESC). We are also grateful for the funding contribution provided by the Space Technology Mission Directorate, Game Changing Development Program, toward the completion of this flight campaign.

REFERENCES

- [1] Ryan, R. and Townsend, J., "Fundamentals and Issues in Launch Vehicle Design," *J. Spacecraft and Rockets*, Vol. 34, No. 2 (1997), pp. 192-198.
- [2] Hickey, C., Loveall, J., Orr, J. K., and Klausman, A., "The Legacy of Space Shuttle Flight Software," *Proc. AIAA Space 2011 Conference*, Long Beach, California, September 2011, AIAA 2011-7307.
- [3] Orr, J., Wall, J., VanZwieten, T., and Hall, C., "Space Launch System Ascent Flight Control Design," American Astronautical Society Guidance, Navigation, and Control Conference, Breckenridge, Colorado, Jan 31-Feb 5, 2014, AAS 14-038.
- [4] VanZwieten, T., Gilligan, E., Wall, J., Orr, J., Miller, C., and Hanson, C., "Adaptive Augmenting Control Flight Characterization Experiment on an F/A-18", *Proc. American Astronautical Society Guidance, Navigation, and Control Conference*, Breckenridge, Colorado, Jan 31-Feb 5, 2014, AAS 14-052.
- [5] Wall, J., VanZwieten, T., Gilligan, E., Miller, C., Hanson, C., and Orr, J., "In-Flight Suppression of an Unstable F/A-18 Structural Mode Using the Space Launch System Adaptive Augmenting Control System," *Proc. 2015 AIAA Guidance, Navigation, and Control Conference*, AIAA-2015-1775.
- [6] Hanson, C., Miller, C., VanZwieten, T., Gilligan, E., Orr, J., and Wall, J., "Launch Vehicle Manual Steering with Adaptive Augmenting Control: In-Flight Evaluations Using a Piloted Aircraft", *Proc. 2015 AIAA Guidance, Navigation, and Control Conference*, AIAA-2015-1776.
- [7] Miller, C., "Nonlinear Dynamic Inversion Baseline Control Law: Architecture and Performance Predictions," *Proc. AIAA Guidance, Navigation, and Control Conference*, 8-11 August 2011, AIAA 2011-6467.
- [8] Miller, C., "Nonlinear Dynamic Inversion Baseline Control Law: Flight-Test Results for the Full-scale Advanced Systems Testbed F/A-18 Airplane," *Proc. AIAA Guidance, Navigation, and Control Conference*, 8-11 August 2011, AIAA 2011-6468.
- [9] Orr, J., Johnson, M., Wetherbee, J., and McDuffie, J., "State Space Implementation of Linear Perturbation Dynamics Equations for Flexible Launch Vehicles," *Proc. AIAA Guidance, Navigation, and Control Conference*, 10-13 August 2009, AIAA 2009-5962.
- [10] Orr, J., "A Flight Dynamics Model for a Multi-Actuated Flexible Rocket Vehicle," *Proc. AIAA Atmospheric Flight Mechanics Conference*, 8-11 August 2011, AIAA 2011-6563.
- [11] Orr, J., "Elastic Model Transitions Using Quadratic Inequality Constrained Least Squares," *Proc. AIAA Modeling and Simulation Technologies Conference*, 13-16 August 2012, AIAA 2012-4561